Search for dark matter from the center of the Earth with 8 years of IceCube data

The IceCube Collaboration

(a complete list of authors can be found at the end of the proceedings)

E-mail: grenzi@icecube.wisc.edu, grenzi@ulb.be

The nature of Dark Matter (DM) remains one of the most important unresolved questions of fundamental physics. Many models, including Weakly Interacting Massive Particles (WIMPs), assume DM to be a particle and predict a weak coupling with Standard Model matter. If DM particles can scatter off nuclei in the vicinity of a massive object such as a star or a planet, they may lose kinetic energy and become gravitationally trapped in the center of such objects, including Earth. As DM accumulates in the center of the Earth, self-annihilation of WIMPs into Standard Model particles can result in an excess of neutrinos which are detectable at the IceCube Neutrino Observatory, situated at the geographic South Pole. A search for excess neutrinos from these annihilations has been performed using 8 years of IceCube data, and results have been interpreted in the context of a number of WIMP annihilation channels ($\chi\chi \to \tau^+\tau^-/W^+W^-/b\bar{b}$) and masses ranging from 10 GeV to 10 TeV. We present the latest results from this analysis and compare the outcome with previous analyses by IceCube and other experiments, showing competitive results, which are even world-leading in some parts of the parameter space.

Corresponding authors: Giovanni Renzi[1]*

[1] *Université Libre de Bruxelles*

* Presenter

1. Introduction

Astronomical evidence for the existence of Dark Matter (DM) has been observed throughout the whole last century. The nature of DM remains unknown and several models have been proposed to describe it [1]. Among others, particle DM models stand out for the number of experiments that have been probing them. The Weakly Interactive Massive Particle (WIMP) is one of the most discussed candidates and is predicted by supersymmetric extensions of the Standard Model (SM). Such particles could scatter off SM particles in the vicinity of a massive celestial body, such as the Sun or the Earth, lose energy and be gravitationally trapped in the center of the body. WIMPs accumulated in this way can self-annihilate into SM particles with a rate that is proportional to the DM density in the center of the body. Neutrinos can be produced in this process and their particular properties allow them to travel through dense environments and for long distances. For the Earth, they can reach the surface of the planet and potentially be detected.

The IceCube Neutrino Observatory can measure the flux of neutrinos coming from the center of the Earth. Previously, a search with 1 year of data [2] has produced upper limits on the spin-independent WIMP-nucleon cross-section. in these proceedings the latest developments on the new search using 8 years of data will be presented.

2. The IceCube detector

IceCube [3] is a cubic kilometer neutrino detector located at the geographic South Pole and installed in the Antarctic ice between depths of 1450 m and 2450 m. The detector consists of a large array of photomultipliers (PMTs) housed in glass spheres called Digital Optical Modules (DOMs). IceCube is composed of 86 vertical strings with 60 DOMs each and vertical spacing of 125 m. The DOMs record Cherenkov light emitted along the path of relativistic charged particles produced by neutrino interactions. The collected light allows reconstruction of the characteristics of the primary neutrinos such as energy and direction. Inside the IceCube volume, a smaller and denser array at a depth of 1750 cm, called DeepCore, is also installed. It consists of 8 closely-spaced strings in the center of the primary array with average sensor spacing of 72 m. DeepCore can use the remaining instrumented volume as a veto against muon and neutrino events originating from atmospheric interactions. DeepCore is of particular importance to detect neutrinos with energy below 100 GeV.

3. Dark matter from the center of the Earth

Dark matter particles can be captured in the center of the Earth when they lose energy by scattering off nucleons in the planet. The relative abundance of elements in the Earth sets the capture process to be led by the spin-independent DM-nucleon cross-section σ_{SI}. The capture rate C_{C} depends further on the DM particle mass and the DM density and velocity distribution in the Solar System. Self-annihilation can thereby happen in the center of the Earth, led by the velocity averaged self-annihilation cross-section $\langle \sigma_A v \rangle$. The full process is described by [4]:

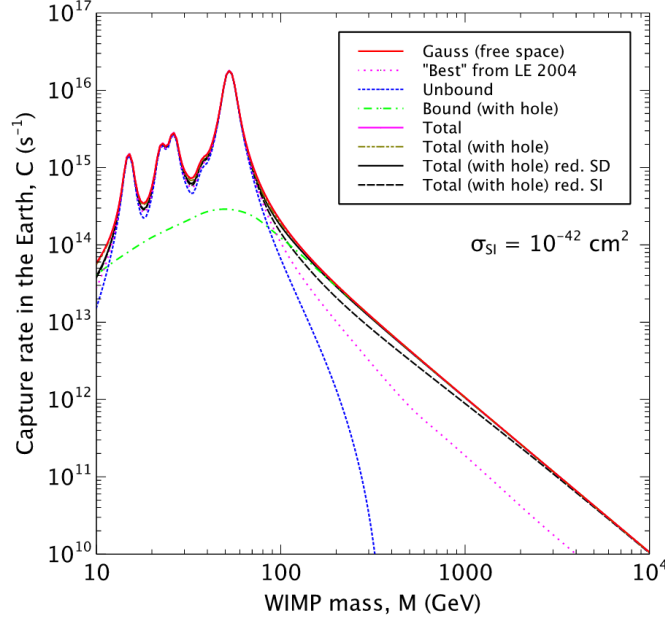$$\dot{N} = C_{\text{C}} - C_{\text{A}}N^2 - C_{\text{E}}N, \tag{1}$$

Figure 1: Capture rate as a function of the DM mass assuming $\sigma_{SI} = 10^{-42}$ cm^2. [8]

where $\Gamma_A = C_A N^2$ is the annihilation rate and depends on $\sigma_A v$ and the age of the Earth $t_\oplus \simeq 4.5 \times 10^9$ y. The evaporation term $C_E N$ can be neglected for masses bigger than a few GeV [5], therefore (1) has solution

$$\Gamma_A = \frac{C_C}{2} \tanh^2 \left(\frac{t}{\tau} \right), \tag{2}$$

where $\tau = (C_C \cdot C_A)^{-1/2}$. (1) reaches equilibrium when $t \gg \tau$. The equilibrium have not reached for the Earth case. This means that, to compute σ_{SI}, a value for $\langle \sigma_A v \rangle$ must be assumed.

The Standard Halo Model (SMH) [6] is the galactic dark matter description adopted for this work. It assumes a truncated Maxwellian velocity distribution with a dispersion of 270 km/s and an escape velocity of 544 km/s. The local DM density value is under debate [7] and could vary between ~ 0.2 GeV/cm^3 and ~ 0.5 GeV/cm^3. For this analysis, in consistency with the other searches in the field, the value 0.3 GeV/cm^3 is assumed.

IceCube can detect the neutrino flux reaching the surface at the South Pole, which can be described by

$$\Phi = \frac{\Gamma_A}{4\pi R_\oplus^2} \frac{dN_\nu}{dE_\nu}, \tag{3}$$

where $R_\oplus$ is the Earth radius and $\frac{dN_\nu}{dE_\nu}$ is neutrino energy spectrum, which depends on the DM particle mas and the annihilation channel.

4. Datasets and event selection

The analysis is intended to use 8 years of IceCube data, from 2011 to 2018. The peculiar position of the source does not allow us to rely on scrambled data to estimate the background, so

Monte-Carlo (MC) simulations are necessary. A burn sample of ~ 204 days of data is used to check the reliability of the simulations, in terms of distributions and overall rates.

The signal for this analysis consists of nearly vertical, up-going tracks, which are produced when the signal neutrinos interact in the instrumented ice volume. The main background for this analysis is the so-called *atmospheric muons*: these are produced in cosmic-ray air showers and cannot traverse the Earth so that from the point of view of IceCube they can only be down-going events. Some of them are though mis-reconstructed as up-going, simulating directions which are typical of the signal. Another relevant background is the *atmospheric neutrinos*, which are produced which are produced in the same interactions which produce atmospheric muons and can traverse the whole Earth. These neutrinos are therefore up-going and interact in the detector in the same way as for signal.

Signal simulations have been obtained with the WimpSim [9] software package, which can produce self-annihilation events in the center of the Earth and propagate them to the detector. In particular, datasets for annihilation channels $\chi\chi \rightarrow \tau^+\tau^-/W^+W^-/b\bar{b}$ and for DM mass from 10 GeV to 10 TeV have been produced. Atmospheric muons have been simulated with CORSIKA [10]. Atmospheric neutrinos are simulated with the NuGen and GENIE software package. Neutrino oscillation [11] has to be taken into account when simulating neutrinos with energies below 100 GeV.

A dedicated event selection has been developed for this analysis. The early stages of the selection are focused on separating muons from neutrinos. This can be achieved by imposing that the interaction producing the track happens in the detector and via some cuts on the quality of the reconstruction; the muons are mis-reconstructed, hence they tend to have lower-quality reconstructions. The main stage of the selection is a random forest classifier. This machine-learning tool can be trained to discriminate signal from background assigning a score from -1 (most background like) to 1 (most signal like). The Boosted Decision Trees (BDTs) constituting the forest are fed the burn sample data as the background set and signal simulation as the signal set. At this point, the selection is split into High Energy (HE) and Low Energy (LE) selections, because events from the highest DM masses have been observed to widely differ from events from the lowest DM masses. The LE selection MC statistics is, at this point, not high enough to allow a proper treatment for the latest stages of the selection. Hence 200 random forests are trained and the events are assigned a weight corresponding to the ratio of random forests that would pass a certain cut on the random forest score. For the HE selection statistics are sufficient to continue the analysis, therefore one only random forest is trained and a straight cut on the score is applied. The two cut values have been chosen to be the values that obtain the best possible sensitivity for the LE and HE selections respectively. The cut value for the LE selection is 0.24 and the weights can hence be expressed as

$$w_{0.24} = \frac{n_{s>0.24}}{n_{\text{tot}}}, \tag{4}$$

where s is the score and $n_{\text{tot}} = 200$. The cut value for the HE selection is $s > 0.18$. Distributions of the scores for the two selections are in figure 2.

The last stage of the selection consists of a hard cut on the reconstructed zenith value at $\theta_{\text{reco}} > 2.8$ rad and the performance of a more suitable energy reconstruction algorithm. It is worth underlining that, at this stage, the atmospheric muon component of the background is completely removed.

4
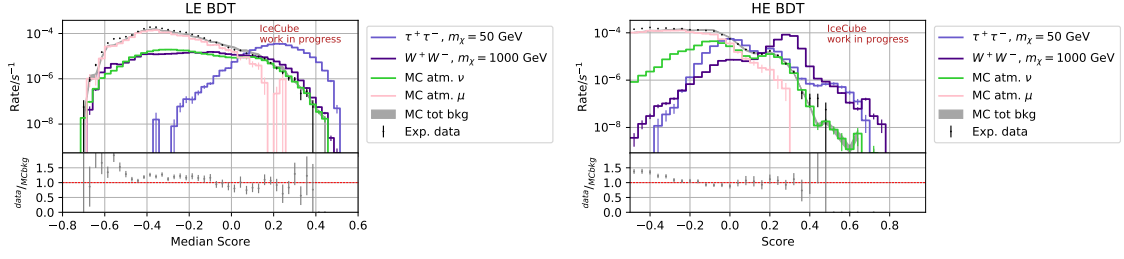
Median score value distributions for the LE selection.   Score value distributions for the HE selection.

Figure 2: The two violet lines indicate the two baseline signal datasets: $\chi\chi \to \tau^+\tau^-$, m_χ = 50 GeV and $\chi\chi \to W^+W^-$, m_χ = 1 TeV for LE and HE respectively. The grey band indicates the total MC distribution. Statistical uncertainties are included.

5. Analysis method and sensitivity

In order to obtain limits, a binned analysis is performed. The Point Spread Function (PDF) is defined for each bin as follows:

$$\mu_{\text{bin}}(\xi, \overrightarrow{\eta}) = \xi S_{\text{bin}}(\theta, E) + \sum_i \eta_i B_{i,\text{bin}}(\theta, E), \tag{5}$$

with N_{tot} being the total number of events, ξ is the signal fraction, η_i are the fractions of the various background component, $S(\theta, E)$ is the final distribution for signal and $B_i(\theta, E)$ are the final distributions of the background components. These are 2D zenith-energy distributions and are shown in figures 3 and 4 for the LE and HE selections respectively. These distributions are the for the analysis. The number of bins representing the data has been optimized to obtain the best possible sensitivities.
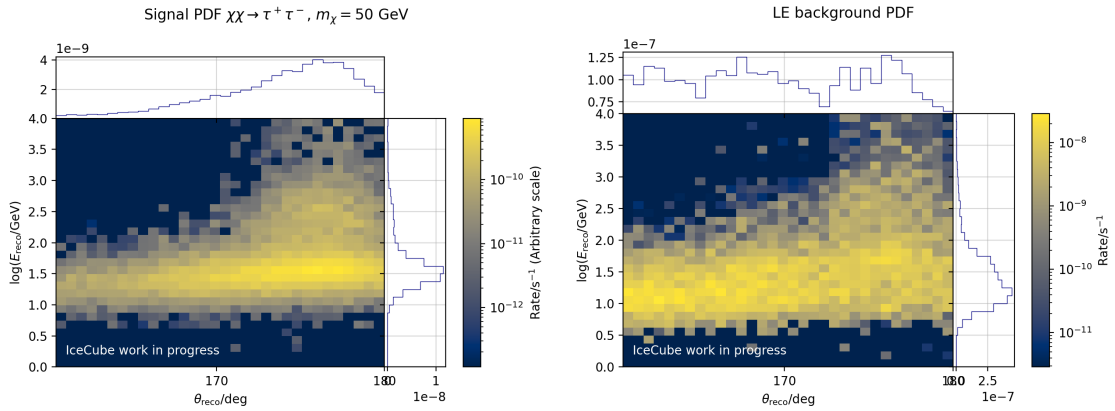

Figure 3: Signal baseline and atmospheric background distribution for the LE selection.

The "effective" likelihood developed in [12] is used. This likelihood expression can be considered a genralization of the Poisson likelihood, where the uncertainties on the distributions are taken into account. In the case where the uncertainties are negligible, it reduces to the Poisson case. Given the signal fraction ξ, the parameters that describe the background $\overrightarrow{\eta}$, and the number
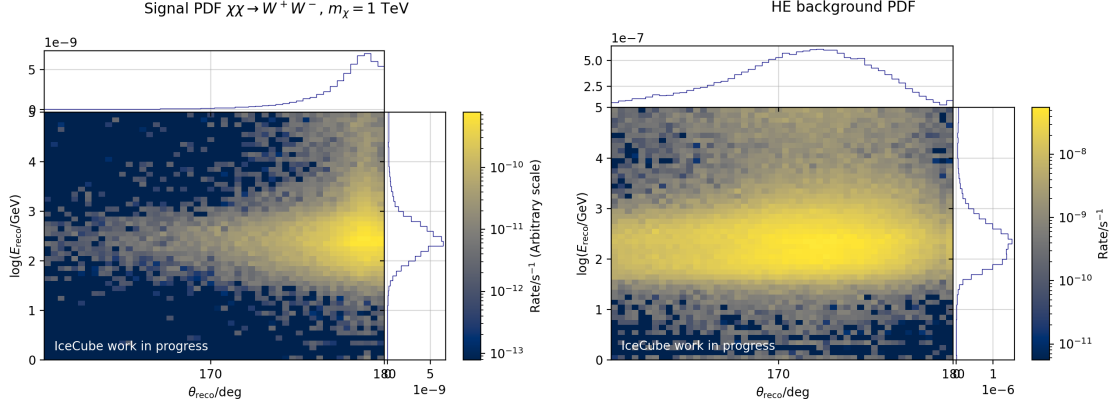
5

Figure 4: Signal baseline and atmospheric background distribution for the LE selection.

of observed events k, the likelihood can be expressed as

$$\mathcal{L}_{\text{eff}}(\mu|k) = N_{\text{tot}} \frac{\beta^{\alpha}\Gamma(k+\alpha)}{k!(1+\beta)^{k+\alpha}\Gamma(\alpha)}, \tag{6}$$

where α and β are functions of the observed distribution μ and its uncertainty distribution σ:

$$\alpha = \frac{\mu^2}{\sigma^2} \;\; ; \;\; \beta = \frac{\mu}{\sigma^2}, \tag{7}$$

The total likelihood is the sum of the likelihoods calculated for each bin.

The Test Statistic (TS) is defined by the ratio of likelihood absolute best fit and the best fit obtained by keeping $\xi = 0$:

$$TS = \frac{\mathcal{L}(\hat{\xi}, \hat{\vec{\eta}}|k)}{\mathcal{L}(\xi = 0, \hat{\hat{\vec{\eta}}}|k)}. \tag{8}$$

The 90% confidence level limit is computed via a frequentist approach. Signal events are progressively injected and pseudo-experiments are generated at each step. A TS is computed for each trial. The limit is reached when, for a certain number of injected signal events $n_{\text{inj}}^{0.9}$, 90% of the pseudo-experiments TS values are greater than the median TS obtained when $n_{\text{inj}} = 0$. $n_{\text{inj}}^{0.9}$ is hence the sensitivity at 90% Confidence Level (C.L.) in terms of number of events.

The volumetric flux limit can be computed as follows:

$$\Gamma_{\nu \to \mu} = \frac{n_{\text{inj}}^{0.9}}{t_{\text{live}}V_{\text{eff}}}, \tag{9}$$

where t_{live} is the livetime of the analysis and V_{eff} the effective volume of the detector. The volumetric fluxes can then be converted to annihilation rates via WimpSim. Capture rate limits can be obtained by solving (2) analytically. As explained in section 3, an assumption on $\langle\sigma_A v\rangle$ must be made. For a fair comparison to other searches in the field, the thermal value $\langle\sigma_A v\rangle = 3 \times 10^{-26}$ cm³s is assumed. Figure 5 shows σ_{SI} in function of $\langle\sigma_A v\rangle$. The final results for σ_{SI} can be found by converting capture rates via WimpSim. Figure 6 illustrates the 90% C.L. sensitivities for σ_{SI} in comparison with other results. For each DM channel and mass combination, the selection giving

the best sensitivity between LE and HE is chosen. The "switch" from LE to HE happens for every channel at $m_\chi \sim 100$ GeV. This analysis sensitivities promise competitive limits, world-leading in the HE selection parameter space.
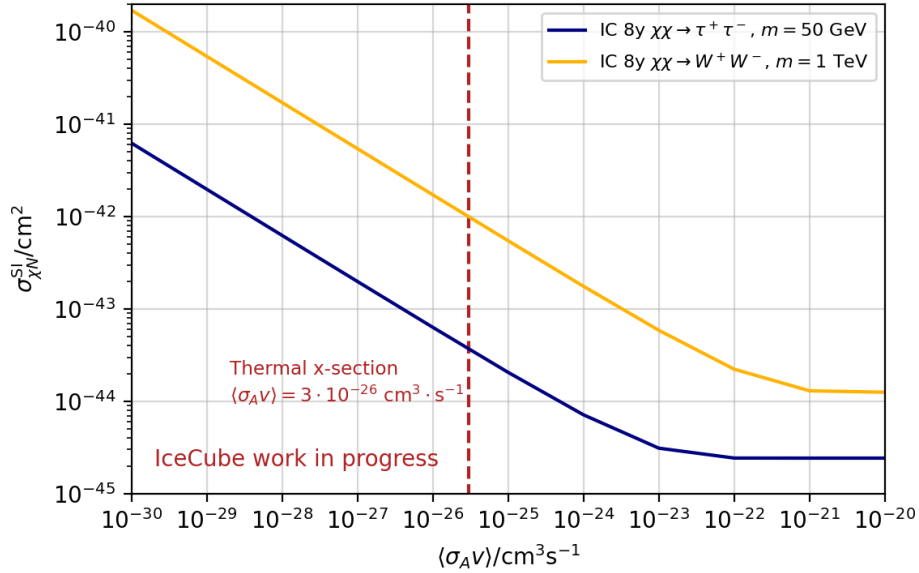

Figure 5: Sensitivity for σ_{SI} in function of the assumption made on $\langle\sigma_A v\rangle$. The lines reach a horizontal plateau when the process is in equilibrium.
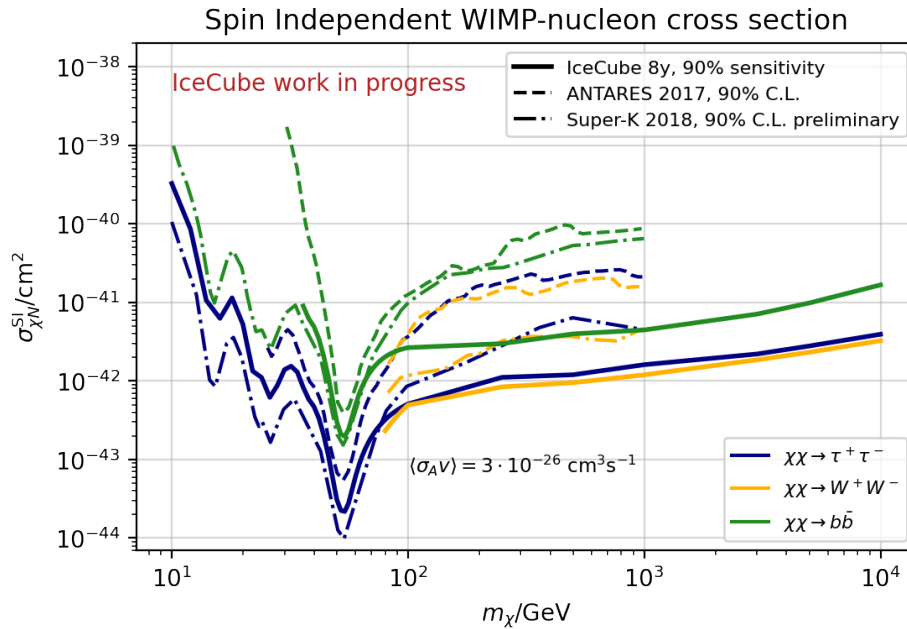

Figure 6: Sensitivities at 90% C.L. compared to the latest results from ANTARES [13] and Super-Kamiokande [14].

6. Conclusions

Sensitivities have been computed for the 8 years search for DM from the center of the Earth. A new likelihood expression has been employed to take into account uncertainties. Adding the energy in 2D distributions with zenith has shown improvements as compared with previous iterations [15] of the analysis which were using zenith distributions only. The analysis setting is in the very latest stages, therefore official results are foreseen to be released soon.

References

[1] G. Bertone, D. Hooper, and J. Silk *Phys.Rept.* **405** (2005) 279–390.

[2] **IceCube** Collaboration, M. G. Aartsen *et al. EPJ C* **77** no. 2, (2017) 82.

[3] **IceCube** Collaboration, M. G. Aartsen *et al. JINST* **12** no. 03, (2017) P03012.

[4] K. Griest and D. Seckel *Nucl. Phys. B* **283** (1987) 681.

[5] R. Garani and S. Palomares-Ruiz.

[6] G. Jungman, M. Kamionkowski, and K. Griest *Phys. Rept.* **267** (1996) 195–373.

[7] J. I. Read *J. Phys. G* **41** no. 6, (2014) .

[8] S. Sivertsson and J. Edsjö *Phys. Rev. D* **85** no. 123514, (2012) .

[9] M. Blennow, J. Edsjö, and T. Ohlsson *JCAP* **WimpSim Neutrino Monte Carlo, http://wimpsim.astroparticle.se/** no. 01, (2008) 021.

[10] D. Heck, J. Knapp, J. Capdevielle, G. Schatz, and T. Thouw *FZKA* **6019** (1998) .

[11] **IceCube** Collaboration, M. G. Aartsen *et al. Phys. Rev. Lett.* **120** (2018) 071801.

[12] C. Argüelles, A. Schneider, and T. Yuan *J. High Energ. Phys.* **30** (2019) .

[13] **ANTARES** Collaboration *Phys. Dark Univ.* **16** (2017) 41–48.

[14] **Super-Kamiokande** Collaboration, P. Mijakowski *Journal of Physics: Conference Series* **1342** (Jan, 2020) 012075.

[15] **IceCube** Collaboration *PoS* **ICRC2019** (2019) 541.

Full Authors List: IceCube Collaboration

R. Abbasi[17], M. Ackermann[59], J. Adams[18], J. A. Aguilar[12], M. Ahlers[22], M. Ahrens[50], C. Alispach[28], A. A. Alves Jr.[31], N. M. Amin[42], R. An[14], K. Andeen[40], T. Anderson[56], G. Anton[26], C. Argüelles[14], Y. Ashida[38], S. Axani[15], X. Bai[46], A. Balagopal V.[38], A. Barbano[28], S. W. Barwick[30], B. Bastian[59], V. Basu[38], S. Baur[12], R. Bay[8], J. J. Beatty[20, 21], K.-H. Becker[58], J. Becker Tjus[11], C. Bellenghi[27], S. BenZvi[48], D. Berley[19], E. Bernardini[59, 60], D. Z. Besson[34, 61], G. Binder[8, 9], D. Bindig[58], E. Blaufuss[19], S. Blot[59], M. Boddenberg[1], F. Bontempo[31], J. Borowka[1], S. Böser[39], O. Botner[57], J. Böttcher[1], E. Bourbeau[22], F. Bradascio[59], J. Braun[38], S. Bron[28], J. Brostean-Kaiser[59], S. Browne[32], A. Burgman[57], R. T. Burley[2], R. S. Busse[41], M. A. Campana[45], E. G. Carnie-Bronca[2], C. Chen[6], D. Chirkin[38], K. Choi[52], B. A. Clark[24], K. Clark[33], L. Classen[41], A. Coleman[42], G. H. Collin[15], J. M. Conrad[15], P. Coppin[13], P. Correa[13], D. F. Cowen[55, 56], R. Cross[48], C. Dappen[1], P. Dave[6], C. De Clercq[13], J. J. DeLaunay[56], H. Dembinski[42], K. Deoskar[50], S. De Ridder[29], A. Desai[38], P. Desiati[38], K. D. de Vries[13], G. de Wasseige[13], M. de With[10], T. DeYoung[24], S. Dharani[1], A. Diaz[15], J. C. Díaz-Vélez[38], M. Dittmer[41], H. Dujmovic[31], M. Dunkman[56], M. A. DuVernois[38], E. Dvorak[46], T. Ehrhardt[39], P. Eller[27], R. Engel[31, 32], H. Erpenbeck[1], J. Evans[19], P. A. Evenson[42], K. L. Fan[19], A. R. Fazely[7], S. Fiedlschuster[26], A. T. Fienberg[56], K. Filimonov[8], C. Finley[50], L. Fischer[59], D. Fox[55], A. Franckowiak[11, 59], E. Friedman[19], A. Fritz[39], P. Fürst[1], T. K. Gaisser[42], J. Gallagher[37], E. Ganster[1], A. Garcia[14], S. Garrappa[59], L. Gerhardt[9], A. Ghadimi[54], C. Glaser[57], T. Glauch[27], T. Glüsenkamp[26], A. Goldschmidt[9], J. G. Gonzalez[42], S. Goswami[54], D. Grant[24], T. Grégoire[56], S. Griswold[48], M. Gündüz[11], C. Günther[1], C. Haack[27], A. Hallgren[57], R. Halliday[24], L. Halve[1], F. Halzen[38], M. Ha Minh[27], K. Hanson[38], J. Hardin[38], A. A. Harnisch[24], A. Haungs[31], S. Hauser[1], D. Hebecker[10], K. Helbing[58], F. Henningsen[27], E. C. Hettinger[24], S. Hickford[58], J. Hignight[25], C. Hill[16], G. C. Hill[2], K. D. Hoffman[19], R. Hoffmann[58], T. Hoinka[23], B. Hokanson-Fasig[38], K. Hoshina[38, 62], F. Huang[56], M. Huber[27], T. Huber[31], K. Hultqvist[50], M. Hünnefeld[23], R. Hussain[38], S. In[52], N. Iovine[12], A. Ishihara[16], M. Jansson[50], G. S. Japaridze[5], M. Jeong[52], B. J. P. Jones[4], D. Kang[31], W. Kang[52], X. Kang[45], A. Kappes[41], D. Kappesser[39], T. Karg[59], M. Karl[27], A. Karle[38], U. Katz[26], M. Kauer[38], M. Kellermann[1], J. L. Kelley[38], A. Kheirandish[56], K. Kin[16], T. Kintscher[59], J. Kiryluk[51], S. R. Klein[8, 9], R. Koirala[42], H. Kolanoski[10], T. Kontrimas[27], L. Köpke[39], C. Kopper[24], S. Kopper[54], D. J. Koskinen[22], P. Koundal[31], M. Kovacevich[45], M. Kowalski[10, 59], T. Kozynets[22], E. Kun[11], N. Kurahashi[45], N. Lad[59], C. Lagunas Gualda[59], J. L. Lanfranchi[56], M. J. Larson[19], F. Lauber[58], J. P. Lazar[14, 38], J. W. Lee[52], K. Leonard[38], A. Leszczyńska[32], Y. Li[56], M. Lincetto[11], Q. R. Liu[38], M. Liubarska[25], E. Lohfink[39], C. J. Lozano Mariscal[41], L. Lu[38], F. Lucarelli[28], A. Ludwig[24, 35], W. Luszczak[38], Y. Lyu[8, 9], W. Y. Ma[59], J. Madsen[38], K. B. M. Mahn[24], Y. Makino[38], S. Mancina[38], I. C. Mariş[12], R. Maruyama[43], K. Mase[16], T. McElroy[25], F. McNally[36], J. V. Mead[22], K. Meagher[38], A. Medina[21], M. Meier[16], S. Meighen-Berger[27], J. Micallef[24], D. Mockler[12], T. Montaruli[28], R. W. Moore[25], R. Morse[38], M. Moulai[15], R. Naab[59], R. Nagai[16], U. Naumann[58], J. Necker[59], L. V. Nguyễn[24], H. Niederhausen[27], M. U. Nisa[24], S. C. Nowicki[24], D. R. Nygren[9], A. Obertacke Pollmann[58], M. Oehler[31], A. Olivas[19], E. O'Sullivan[57], H. Pandya[42], D. V. Pankova[56], N. Park[33], G. K. Parker[4], E. N. Paudel[42], L. Paul[40], C. Pérez de los Heros[57], L. Peters[1], J. Peterson[38], S. Philippen[1], D. Pieloth[23], S. Pieper[58], M. Pittermann[32], A. Pizzuto[38], M. Plum[40], Y. Popovych[39], A. Porcelli[29], M. Prado Rodriguez[38], P. B. Price[8], B. Pries[24], G. T. Przybylski[9], C. Raab[12], A. Raissi[18], M. Rameez[22], K. Rawlins[3], I. C. Rea[27], A. Rehman[42], P. Reichherzer[11], R. Reimann[1], G. Renzi[12], E. Resconi[27], S. Reusch[59], W. Rhode[23], M. Richman[45], B. Riedel[38], E. J. Roberts[2], S. Robertson[8, 9], G. Roellinghoff[52], M. Rongen[39], C. Rott[49, 52], T. Ruhe[23], D. Ryckbosch[29], D. Rysewyk Cantu[24], I. Safa[14, 38], J. Saffer[32], S. E. Sanchez Herrera[24], A. Sandrock[23], J. Sandroos[39], M. Santander[54], S. Sarkar[44], S. Sarkar[25], K. Satalecka[59], M. Scharf[1], M. Schaufel[1], H. Schieler[31], S. Schindler[26], P. Schlunder[23], T. Schmidt[19], A. Schneider[38], J. Schneider[26], F. G. Schröder[31, 42], L. Schumacher[27], G. Schwefer[1], S. Sclafani[45], D. Seckel[42], S. Seunarine[47], A. Sharma[57], S. Shefali[32], M. Silva[38], B. Skrzypek[14], B. Smithers[4], R. Snihur[38], J. Soedingrekso[23], D. Soldin[42], C. Spannfellner[27], G. M. Spiczak[47], C. Spiering[59, 61], J. Stachurska[59], M. Stamatikos[21], T. Stanev[42], R. Stein[59], J. Stettner[1], A. Steuer[39], T. Stezelberger[9], T. Stürwald[58], T. Stuttard[22], G. W. Sullivan[19], I. Taboada[6], F. Tenholt[11], S. Ter-Antonyan[7], S. Tilav[42], F. Tischbein[1], K. Tollefson[24], L. Tomankova[11], C. Tönnis[53], S. Toscano[12], D. Tosi[38], A. Trettin[59], M. Tselengidou[26], C. F. Tung[6], A. Turcati[27], R. Turcotte[31], C. F. Turley[56], J. P. Twagirayezu[24], B. Ty[38], M. A. Unland Elorrieta[41], N. Valtonen-Mattila[57], J. Vandenbroucke[38], N. van Eijndhoven[13], D. Vannerom[15], J. van Santen[59], S. Verpoest[29], M. Vraeghe[29], C. Walck[50], T. B. Watson[4], C. Weaver[24], P. Weigel[15], A. Weindl[31], M. J. Weiss[56], J. Weldert[39], C. Wendt[38], J. Werthebach[23], M. Weyrauch[32], N. Whitehorn[24, 35], C. H. Wiebusch[1], D. R. Williams[54], M. Wolf[27], K. Woschnagg[8], G. Wrede[26], J. Wulff[11], X. W. Xu[7], Y. Xu[51], J. P. Yanez[25], S. Yoshida[16], S. Yu[24], T. Yuan[38], Z. Zhang[51]

[1] III. Physikalisches Institut, RWTH Aachen University, D-52056 Aachen, Germany

[2] Department of Physics, University of Adelaide, Adelaide, 5005, Australia

[3] Dept. of Physics and Astronomy, University of Alaska Anchorage, 3211 Providence Dr., Anchorage, AK 99508, USA

[4] Dept. of Physics, University of Texas at Arlington, 502 Yates St., Science Hall Rm 108, Box 19059, Arlington, TX 76019, USA

[5] CTSPS, Clark-Atlanta University, Atlanta, GA 30314, USA

[6] School of Physics and Center for Relativistic Astrophysics, Georgia Institute of Technology, Atlanta, GA 30332, USA

[7] Dept. of Physics, Southern University, Baton Rouge, LA 70813, USA

[8] Dept. of Physics, University of California, Berkeley, CA 94720, USA

[9] Lawrence Berkeley National Laboratory, Berkeley, CA 94720, USA

[10] Institut für Physik, Humboldt-Universität zu Berlin, D-12489 Berlin, Germany

[11] Fakultät für Physik & Astronomie, Ruhr-Universität Bochum, D-44780 Bochum, Germany

[12] Université Libre de Bruxelles, Science Faculty CP230, B-1050 Brussels, Belgium

[13] Vrije Universiteit Brussel (VUB), Dienst ELEM, B-1050 Brussels, Belgium

[14] Department of Physics and Laboratory for Particle Physics and Cosmology, Harvard University, Cambridge, MA 02138, USA

[15] Dept. of Physics, Massachusetts Institute of Technology, Cambridge, MA 02139, USA

[16] Dept. of Physics and Institute for Global Prominent Research, Chiba University, Chiba 263-8522, Japan

[17] Department of Physics, Loyola University Chicago, Chicago, IL 60660, USA

[18] Dept. of Physics and Astronomy, University of Canterbury, Private Bag 4800, Christchurch, New Zealand

[19] Dept. of Physics, University of Maryland, College Park, MD 20742, USA

[20] Dept. of Astronomy, Ohio State University, Columbus, OH 43210, USA

[21] Dept. of Physics and Center for Cosmology and Astro-Particle Physics, Ohio State University, Columbus, OH 43210, USA

[22] Niels Bohr Institute, University of Copenhagen, DK-2100 Copenhagen, Denmark

[23] Dept. of Physics, TU Dortmund University, D-44221 Dortmund, Germany

[24] Dept. of Physics and Astronomy, Michigan State University, East Lansing, MI 48824, USA

[25] Dept. of Physics, University of Alberta, Edmonton, Alberta, Canada T6G 2E1

[26] Erlangen Centre for Astroparticle Physics, Friedrich-Alexander-Universität Erlangen-Nürnberg, D-91058 Erlangen, Germany

[27] Physik-department, Technische Universität München, D-85748 Garching, Germany

[28] Département de physique nucléaire et corpusculaire, Université de Genève, CH-1211 Genève, Switzerland

[29] Dept. of Physics and Astronomy, University of Gent, B-9000 Gent, Belgium

[30] Dept. of Physics and Astronomy, University of California, Irvine, CA 92697, USA

[31] Karlsruhe Institute of Technology, Institute for Astroparticle Physics, D-76021 Karlsruhe, Germany

[32] Karlsruhe Institute of Technology, Institute of Experimental Particle Physics, D-76021 Karlsruhe, Germany

[33] Dept. of Physics, Engineering Physics, and Astronomy, Queen's University, Kingston, ON K7L 3N6, Canada

[34] Dept. of Physics and Astronomy, University of Kansas, Lawrence, KS 66045, USA

[35] Department of Physics and Astronomy, UCLA, Los Angeles, CA 90095, USA

[36] Department of Physics, Mercer University, Macon, GA 31207-0001, USA

[37] Dept. of Astronomy, University of Wisconsin–Madison, Madison, WI 53706, USA

[38] Dept. of Physics and Wisconsin IceCube Particle Astrophysics Center, University of Wisconsin–Madison, Madison, WI 53706, USA

[39] Institute of Physics, University of Mainz, Staudinger Weg 7, D-55099 Mainz, Germany

[40] Department of Physics, Marquette University, Milwaukee, WI, 53201, USA

[41] Institut für Kernphysik, Westfälische Wilhelms-Universität Münster, D-48149 Münster, Germany

[42] Bartol Research Institute and Dept. of Physics and Astronomy, University of Delaware, Newark, DE 19716, USA

[43] Dept. of Physics, Yale University, New Haven, CT 06520, USA

[44] Dept. of Physics, University of Oxford, Parks Road, Oxford OX1 3PU, UK

[45] Dept. of Physics, Drexel University, 3141 Chestnut Street, Philadelphia, PA 19104, USA

[46] Physics Department, South Dakota School of Mines and Technology, Rapid City, SD 57701, USA

[47] Dept. of Physics, University of Wisconsin, River Falls, WI 54022, USA

[48] Dept. of Physics and Astronomy, University of Rochester, Rochester, NY 14627, USA

[49] Department of Physics and Astronomy, University of Utah, Salt Lake City, UT 84112, USA

[50] Oskar Klein Centre and Dept. of Physics, Stockholm University, SE-10691 Stockholm, Sweden

[51] Dept. of Physics and Astronomy, Stony Brook University, Stony Brook, NY 11794-3800, USA

[52] Dept. of Physics, Sungkyunkwan University, Suwon 16419, Korea

[53] Institute of Basic Science, Sungkyunkwan University, Suwon 16419, Korea

[54] Dept. of Physics and Astronomy, University of Alabama, Tuscaloosa, AL 35487, USA

[55] Dept. of Astronomy and Astrophysics, Pennsylvania State University, University Park, PA 16802, USA

[56] Dept. of Physics, Pennsylvania State University, University Park, PA 16802, USA

[57] Dept. of Physics and Astronomy, Uppsala University, Box 516, S-75120 Uppsala, Sweden

[58] Dept. of Physics, University of Wuppertal, D-42119 Wuppertal, Germany

[59] DESY, D-15738 Zeuthen, Germany

[60] Università di Padova, I-35131 Padova, Italy

[61] National Research Nuclear University, Moscow Engineering Physics Institute (MEPhI), Moscow 115409, Russia

[62] Earthquake Research Institute, University of Tokyo, Bunkyo, Tokyo 113-0032, Japan

Acknowledgements